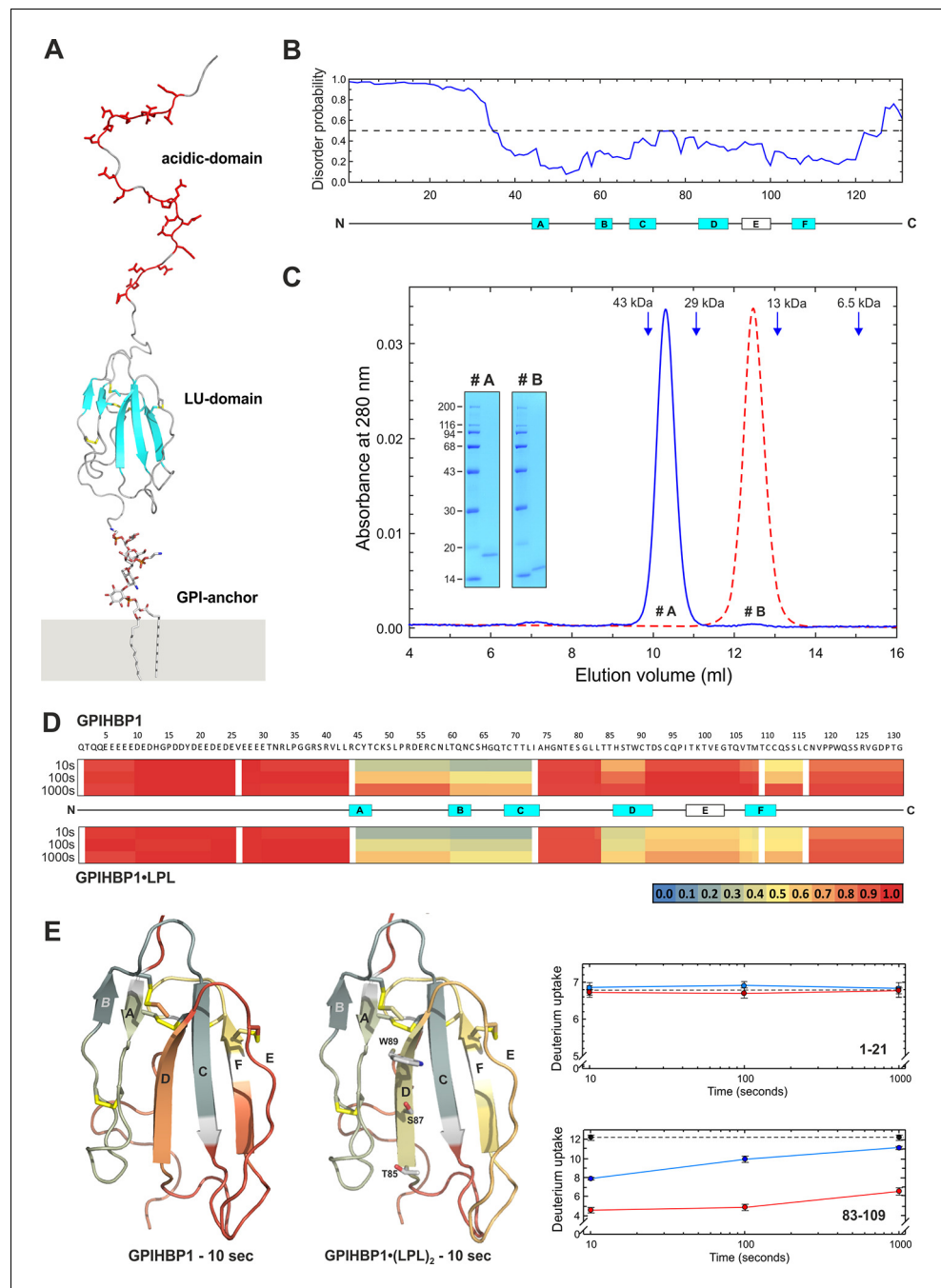


---

## Figures and figure supplements

The acidic domain of the endothelial membrane protein GPIHBP1 stabilizes lipoprotein lipase activity by preventing unfolding of its catalytic domain

**Simon Mysling *et al***



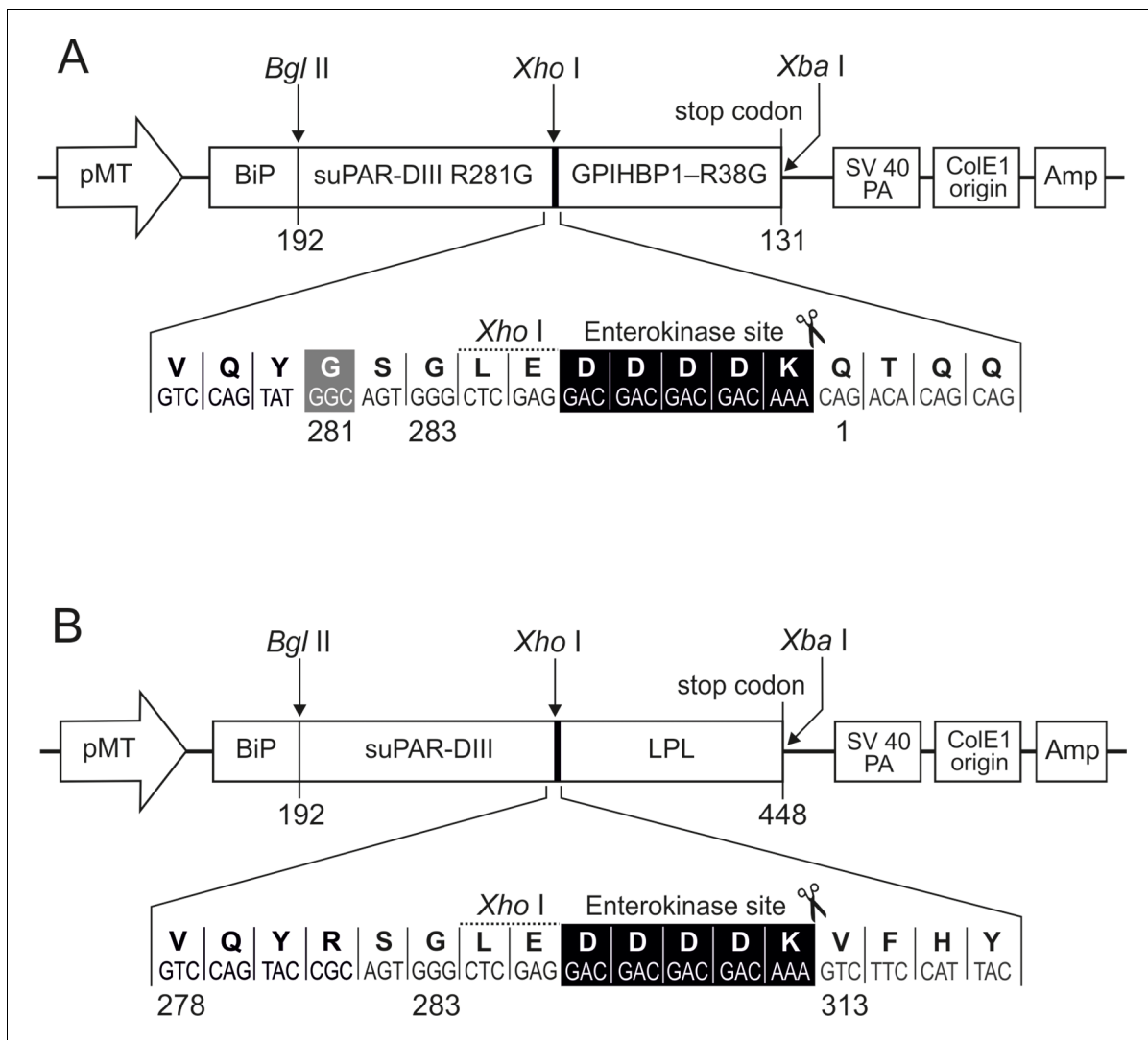
**Figure 1.** Model of human GPIHBP1. Panel **A** shows a cartoon representation for glycolipid-anchored human GPIHBP1. Predicted  $\beta$ -sheets are shown in cyan; acidic amino acid residues in the N-terminal domain are highlighted by red sticks; and the consensus disulfide bonds are shown in yellow. Panel **B** shows a “disorder prediction” for human GPIHBP1 sequence based on the IUPred algorithm. Locations of the six strands of the three-fingered-fold of the LU domain are highlighted by boxes (A–F); strands predicted to form  $\beta$ -sheets are colored cyan. Panel **C** documents the homogeneity and monomer status of purified GPIHBP1<sup>1–131/R38G</sup> (#A) and GPIHBP1<sup>34–131/R38G</sup> (#B) by analytical size-exclusion chromatography with a Superdex HR75 column operated with 20 mM NaH<sub>2</sub>PO<sub>4</sub> and 150 mM NaCl (pH 7.2) and SDS-PAGE (*inset*). Elution positions of the calibration standards are indicated by blue arrows: ovalbumin (43 kDa), carbonic anhydrase (29 kDa), ribonuclease (13 kDa), and aprotinin (6.5 kDa). Panel **D** provides a heat map representation of the relative deuterium uptakes (relative to a fully exchanged control) in peptic peptides from free and LPL-occupied GPIHBP1<sup>1–131</sup> as assessed by HDX-MS. Deuterium uptake was measured after 10, 100, and 1000 s incubations in D<sub>2</sub>O, and relative deuterium uptake is

Figure 1 continued on next page

*Figure 1 continued*

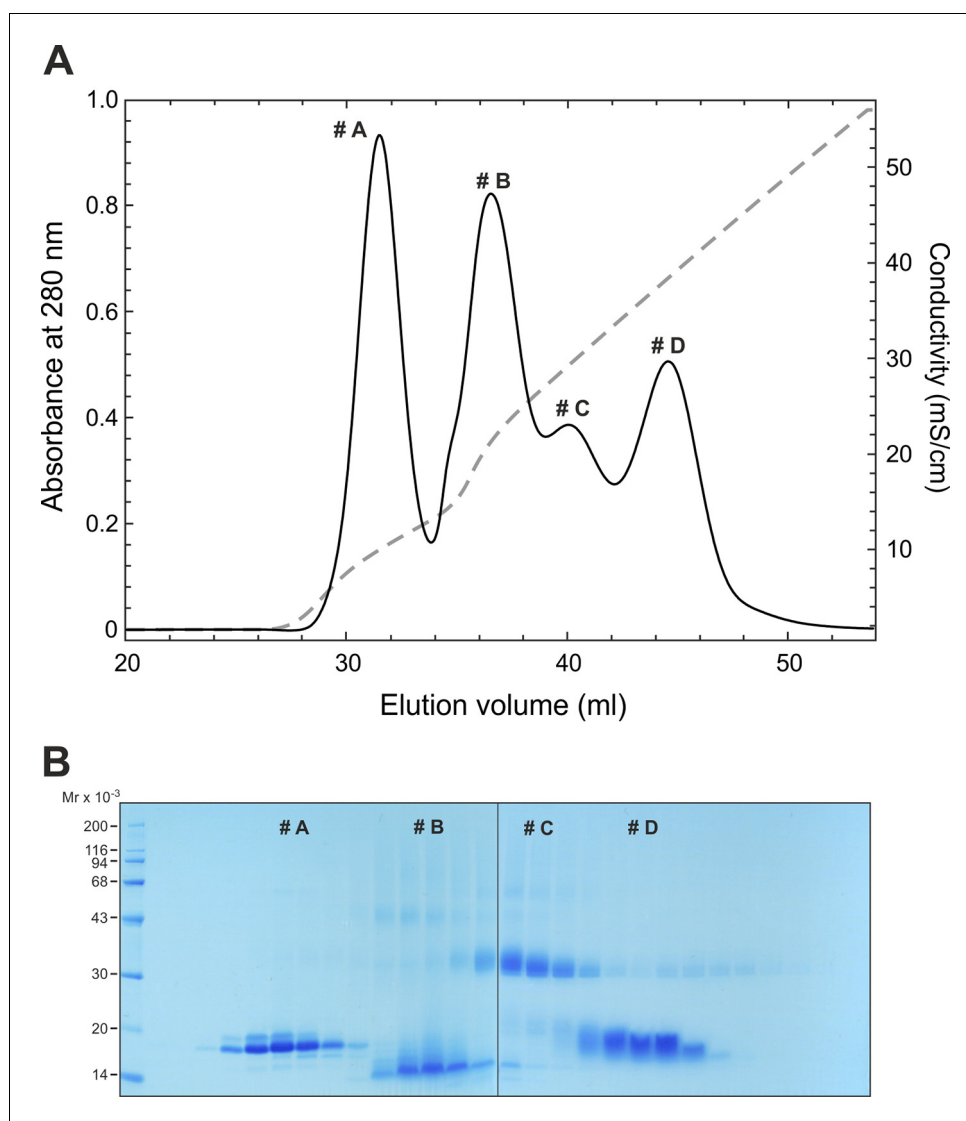
assigned according to the color code (ranging from *blue*, no deuterium uptake, to *red*, full deuterium uptake). A cartoon representation of the differential deuterium uptake for the LU domain between free and LPL-occupied GPIHBP1 after a 10-s exchange is shown in panel **E**. Shown as sticks are the positions of Thr<sup>85</sup>, Ser<sup>87</sup>, and Trp<sup>89</sup> in  $\beta$ -strand D of GPIHBP1. Raw deuterium uptake values for peptides 1–21 and 83–109 are shown for free and LPL-occupied GPIHBP1 (*blue* and *red* solid lines, respectively). The dashed line represents a “full deuteration” control. GPI, glycosylphosphatidylinositol; MS, hydrogen–deuterium exchange mass spectrometry; LU, Ly6/uPAR; SDS-PAGE, sodium dodecyl sulfate polyacrylamide gel electrophoresis

DOI: [10.7554/eLife.12095.003](https://doi.org/10.7554/eLife.12095.003)



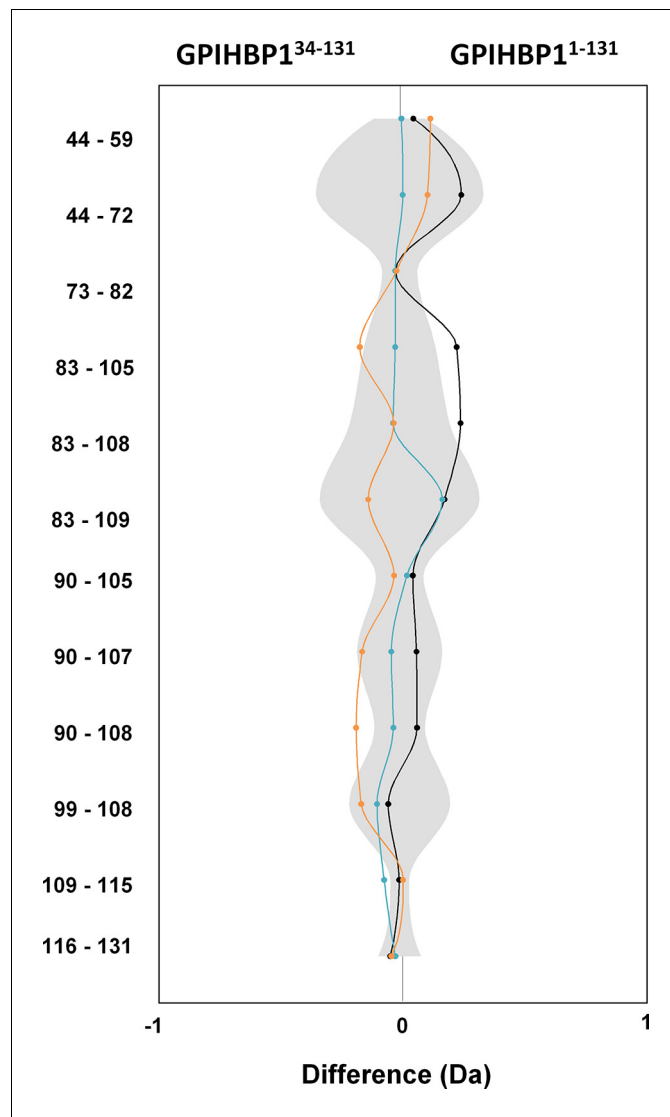
**Figure 1—figure supplement 1.** Constructs encoding soluble DIII-ent-hGPIHBP1<sup>1–131/R38G</sup> and DIII-ent-hLPL<sup>313–448</sup>. Schematic representation of the vectors used for *Drosophila* S2 cell expression of a soluble, secreted human GPIHBP1<sup>1–131</sup> (panel A) and the CTD<sup>313–448</sup> of human LPL (panel B). Both constructs use the third LU domain from human uPAR (DIII<sup>192–283</sup>) as an N-terminal purification tag as described (Gårdsvoll et al., 2013). The enterokinase cleavage site used to excise the recombinant protein (and remove the uPAR tag) is highlighted in black. pMT and BiP represent the *Drosophila* metallothionein promoter and secretion signals, respectively. To optimize enterokinase-mediated excision of GPIHBP1, two mutations (DIII<sup>R281G</sup> and GPIHBP1<sup>R38G</sup>) were introduced to silence two undesired cleavage sites for enterokinase. In the GPIHBP1 construct, the N-terminal signal peptide and the C-terminal hydrophobic peptide required for glycolipid anchoring have been omitted.

DOI: [10.7554/eLife.12095.004](https://doi.org/10.7554/eLife.12095.004)



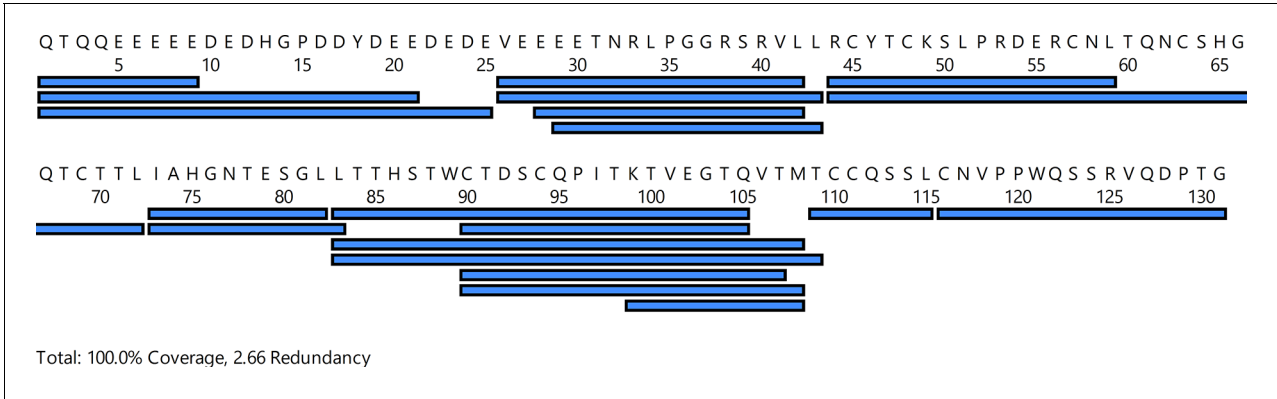
**Figure 1—figure supplement 2.** Purification of recombinant soluble human GPIHBP1<sup>1–131/R38G</sup> and GPIHBP1<sup>34–131/R38G</sup>. Panel A shows a cation-exchange chromatography elution profile for 30 mg of purified DIII-ent-GPIHBP1<sup>1–131/R38G</sup> after enterokinase cleavage. We used a 5 ml HiTrap SP FF column and a 35-ml linear gradient from 0 to 1.0 M NaCl in 50 mM CH<sub>3</sub>COOH, pH 4.5. The peaks correspond to: intact GPIHBP1<sup>1–131/R38G</sup> (#A), GPIHBP1<sup>34–131/R38G</sup> (#B), uncleaved fusion protein (#C) and the excised uPAR DIII tag (#D), as judged by SDS-PAGE of reduced and alkylated samples (panel B) and mass spectrometry (not shown). SDS-PAGE, sodium dodecyl sulfate polyacrylamide gel electrophoresis.

DOI: [10.7554/eLife.12095.005](https://doi.org/10.7554/eLife.12095.005)

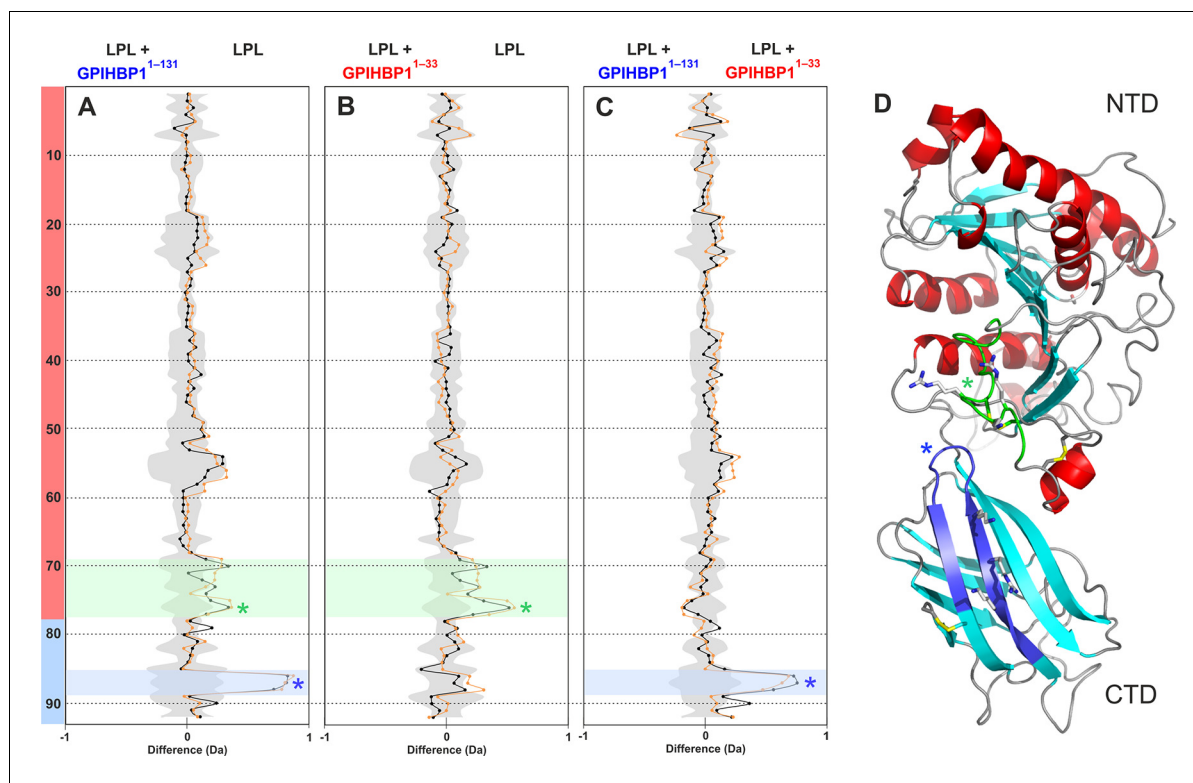


**Figure 1—figure supplement 3.** Comparison of the dynamics in GPIHBP1<sup>34-131</sup> and GPIHBP1<sup>1-131</sup> in HDX-MS experiments. Differential deuterium uptake between intact GPIHBP1<sup>1-131</sup> and GPIHBP1<sup>34-131</sup> (a truncated GPIHBP1 lacking the N-terminal acidic domain) measured by HDX-MS at 25°C is shown as a butterfly plot. Deuterium uptake was traced for 10- (orange), 100- (black), and 1000-sec (blue). The shaded gray area corresponds to the largest standard deviation of the data sets recorded for each peptide. Data points represent the mean of triplicate measurements.

DOI: [10.7554/eLife.12095.006](https://doi.org/10.7554/eLife.12095.006)

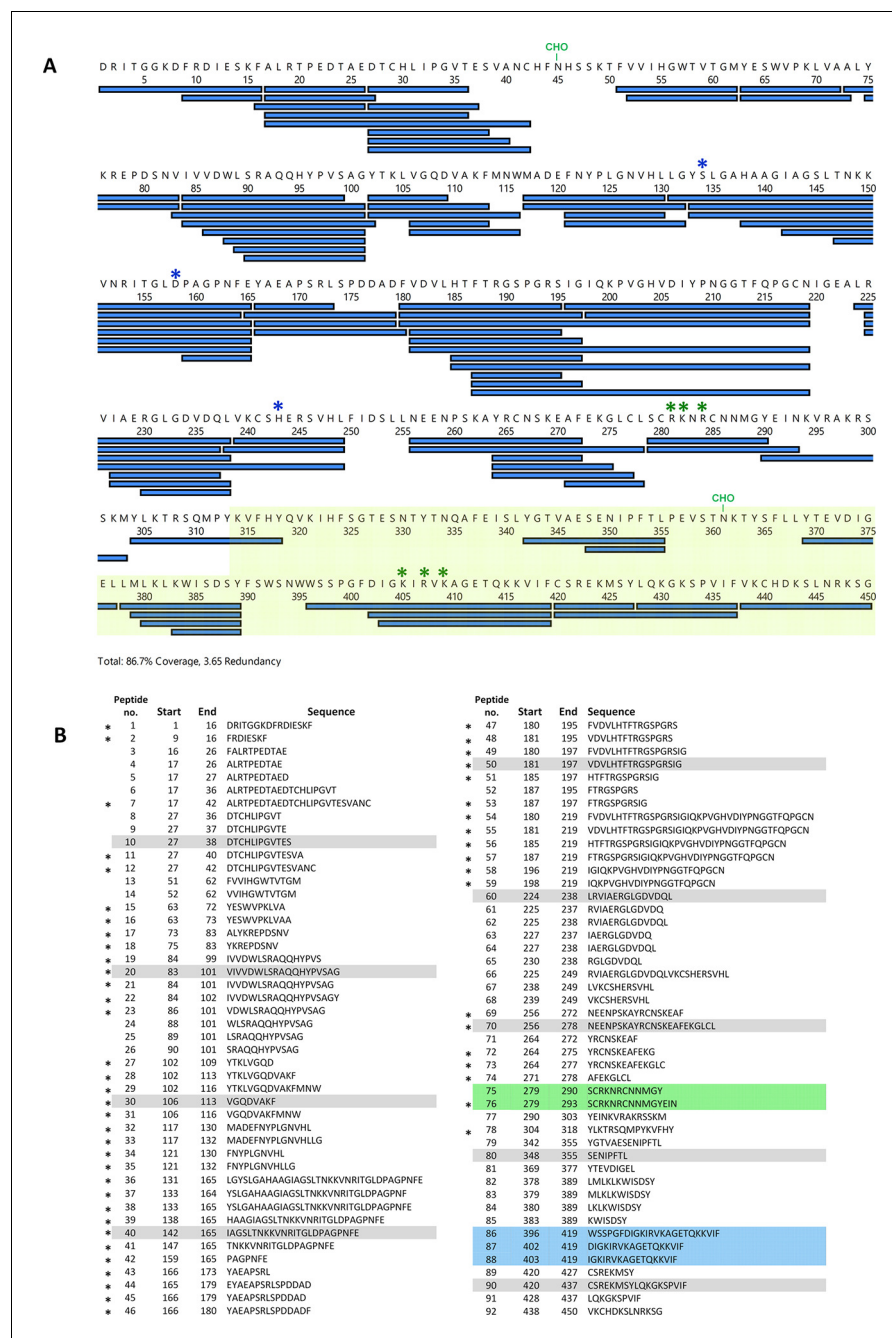


**Figure 1—figure supplement 4.** Peptide list for pepsin-treated GPIHBP1. Peptides recovered after HDX and pepsin cleavage of recombinant human GPIHBP1 are shown as blue bars. HDX, hydrogen–deuterium exchange.  
[DOI: 10.7554/eLife.12095.007](https://doi.org/10.7554/eLife.12095.007)



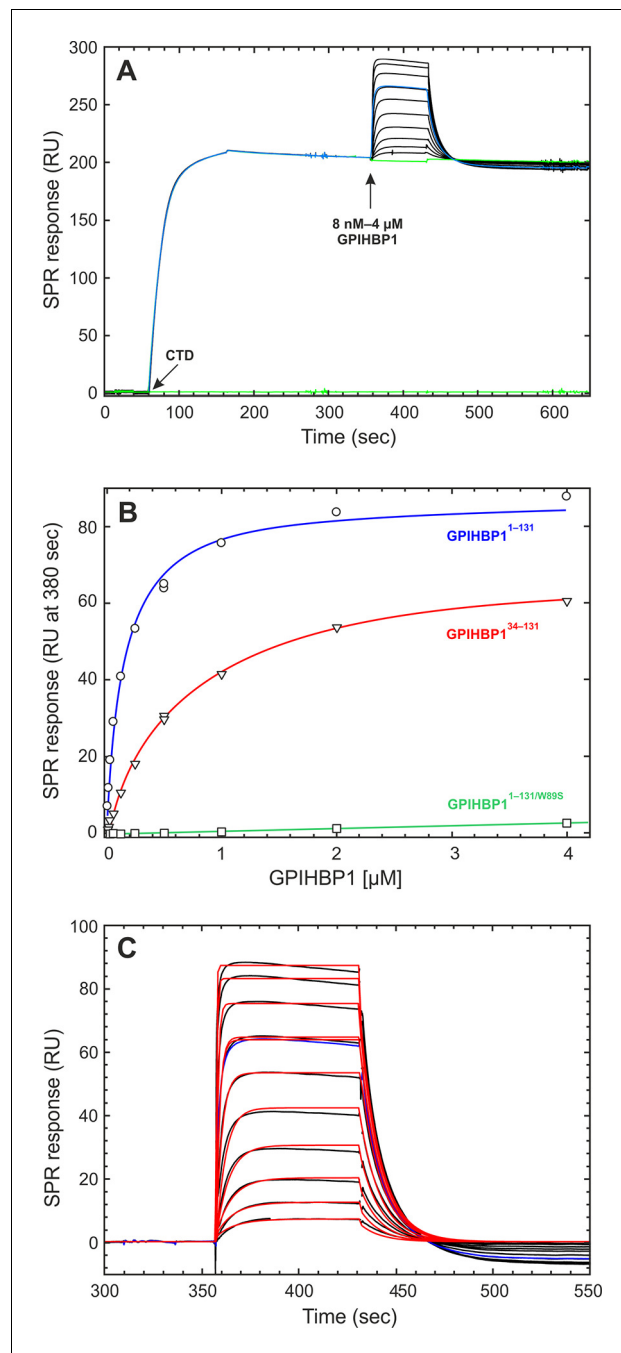
**Figure 2.** Mapping GPIHBP1 interaction sites on LPL. Differential deuterium uptake values for free LPL and LPL occupied with intact GPIHBP1<sup>1-131</sup> (panel A) or the acidic domain peptide GPIHBP1<sup>1-33</sup> (panel B) are shown as butterfly representations. The butterfly plot in panel C compares LPL occupied with GPIHBP1<sup>1-131</sup> or GPIHBP1<sup>1-33</sup>. Due to inherent instability of LPL homodimers, the deuterium uptake was only examined at 10- (orange) and 100-s (black) incubations. The data points represent the mean of triplicate measurements, and the shaded gray area corresponds to the largest standard deviation in the data sets recorded for each peptide. A total of 92 peptides were recovered from LPL, and they are numbered consecutively from the N-terminus. The sequences of the individual peptides are found in **Figure 2—figure supplement 1B**. The transparent red and cyan colors on the left in panel A localize peptides to either the NTD or the CTD domains of LPL, respectively. Panel D shows a cartoon representation of human LPL. Two regions having the most pronounced changes in deuterium uptake with GPIHBP1 binding are highlighted in green (residues 279–293) and blue (residues 402–419); basic residues are shown as sticks. CTD, C-terminal domain; LPL, lipoprotein lipase; NTD, N-terminal domain.

DOI: [10.7554/eLife.12095.008](https://doi.org/10.7554/eLife.12095.008)



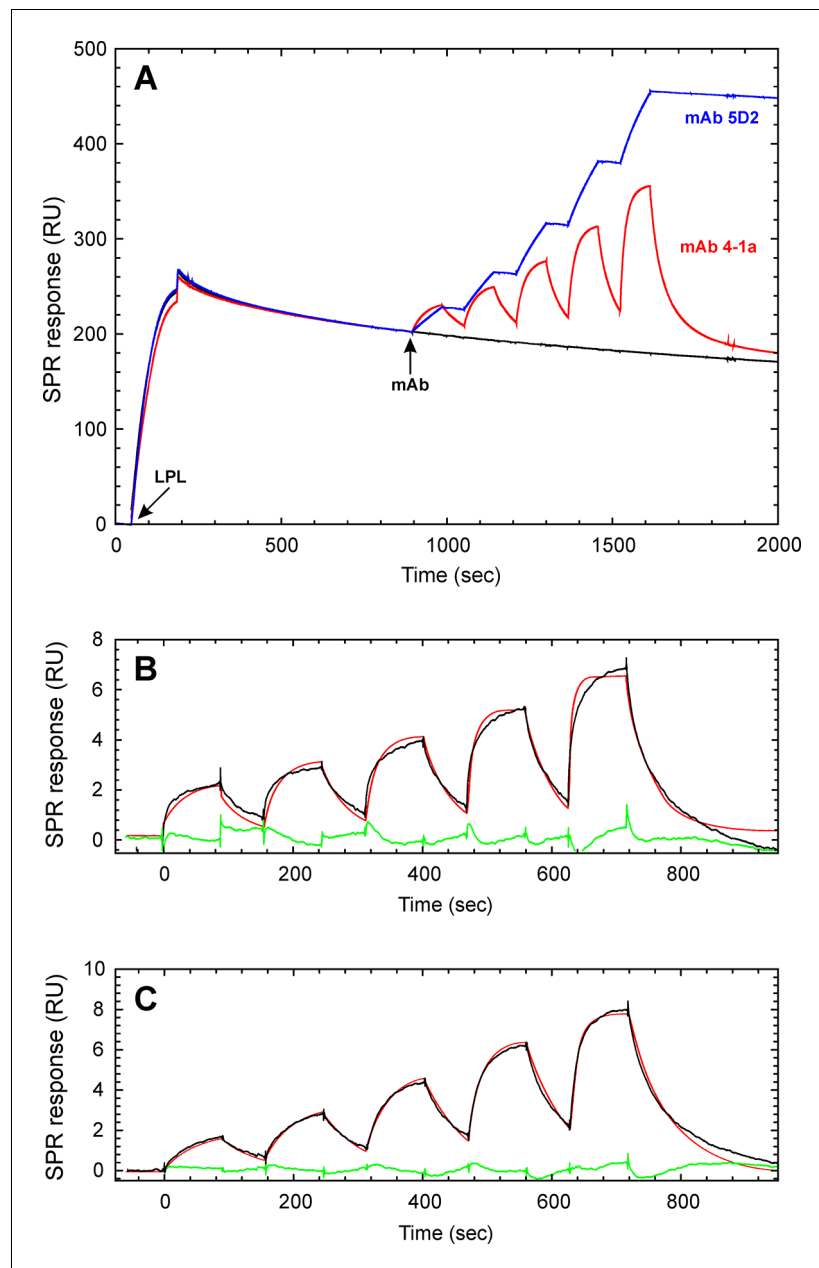
**Figure 2—figure supplement 1.** Peptide list for pepsin-treated bovine LPL. Panel A shows peptides recovered in the HDX-MS studies. Peptides recovered from bovine LPL after pepsin cleavage are shown as blue bars. The CTD is highlighted by the transparent light green box; N-linked glycosylation sites are shown (CHO); residues forming the catalytic triad are indicated by blue asterisks; heparin-binding sequences are shown by green asterisks. Panel B shows the inventory of 92 peptides recovered from LPL. Peptides designated with an asterisk display a bimodality of their isotopic envelopes after a 45-min incubation in H<sub>2</sub>O-buffers followed by 10 and 100 s incubations in D<sub>2</sub>O buffers (as illustrated for the peptic peptide 131–165 in **Figure 6A**). CHO, carbohydrate; CTD, C-terminal domain; HDX-MS, hydrogen–deuterium exchange mass spectrometry; LPL, lipoprotein lipase.

DOI: 10.7554/eLife.12095.009



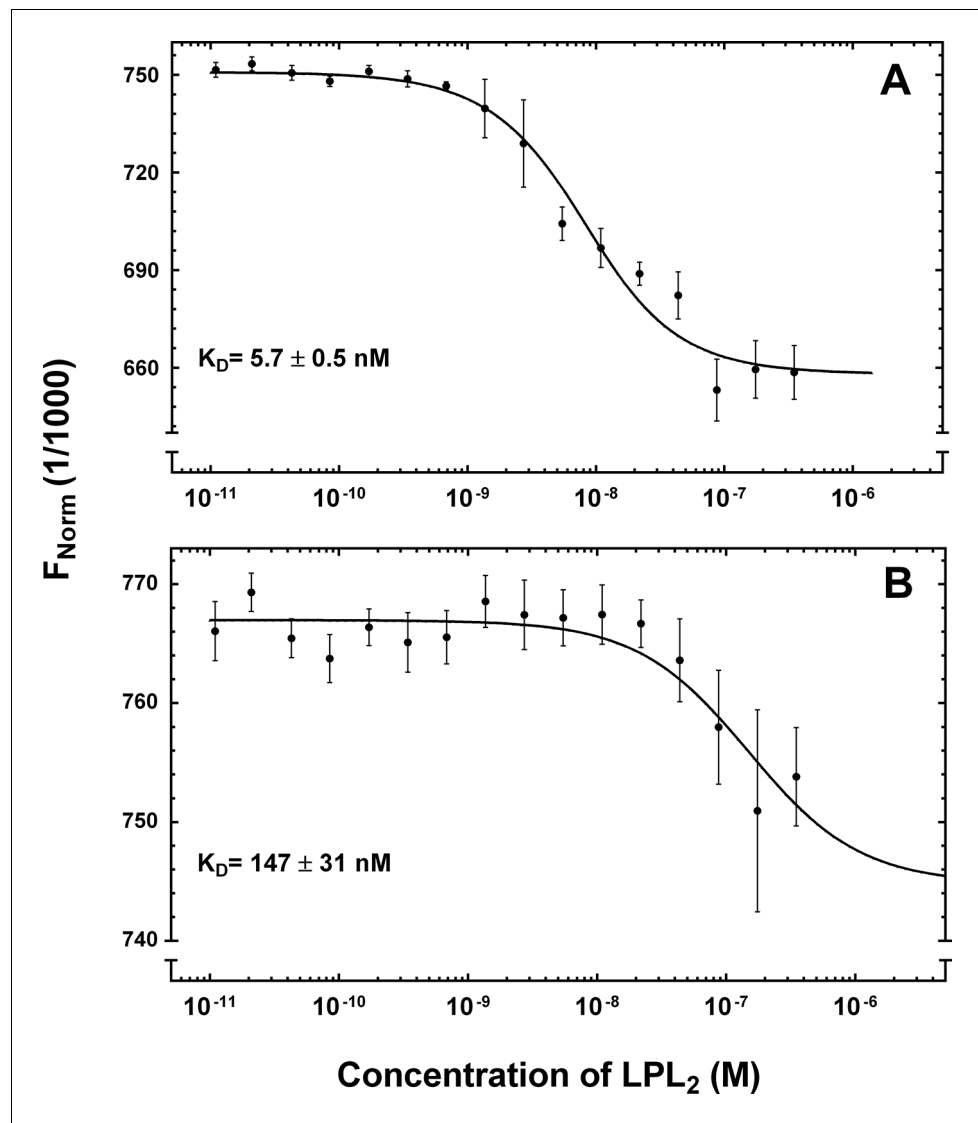
**Figure 3.** Real-time binding kinetics for the interaction between GPIHBP1 and the CTD of human LPL. Panel **A** shows repeat binding of 100 nM of recombinant CTD<sup>313–448</sup> from human LPL to immobilized mAb 5D2 followed by multi-cycle injections of twofold dilutions of GPIHBP1<sup>1–131</sup> (black lines). The green line represents a buffer control; the blue line represents a repeat injection of 250 nM GPIHBP1 at the end of the experiment to demonstrate reproducibility. Panel **B** shows equilibrium binding isotherms for the interactions between the immobilized CTD of LPL and GPIHBP1<sup>1–131</sup> (blue), GPIHBP1<sup>34–131</sup> (red), and GPIHBP1<sup>1–131/W89S</sup> (green) with the SPR signal at 380 s in panel **A** as equilibrium binding level. Panel **C** shows a kinetic evaluation of the double-referenced SPR data for GPIHBP1<sup>1–131</sup> with a global fit to a 1:1 binding model (fits shown in red). Note there is a slight decay of the binding signal at equilibrium due to a weak ligand-induced dissociation of the CTD from mAb 5D2; this effect translates into dissociation below baseline for the higher concentration of GPIHBP1<sup>1–131</sup>. These effects were not observed for GPIHBP1<sup>34–131</sup>. CTD, C-terminal domain; LPL, lipoprotein lipase; SPR, surface plasmon resonance.

DOI: [10.7554/eLife.12095.011](https://doi.org/10.7554/eLife.12095.011)



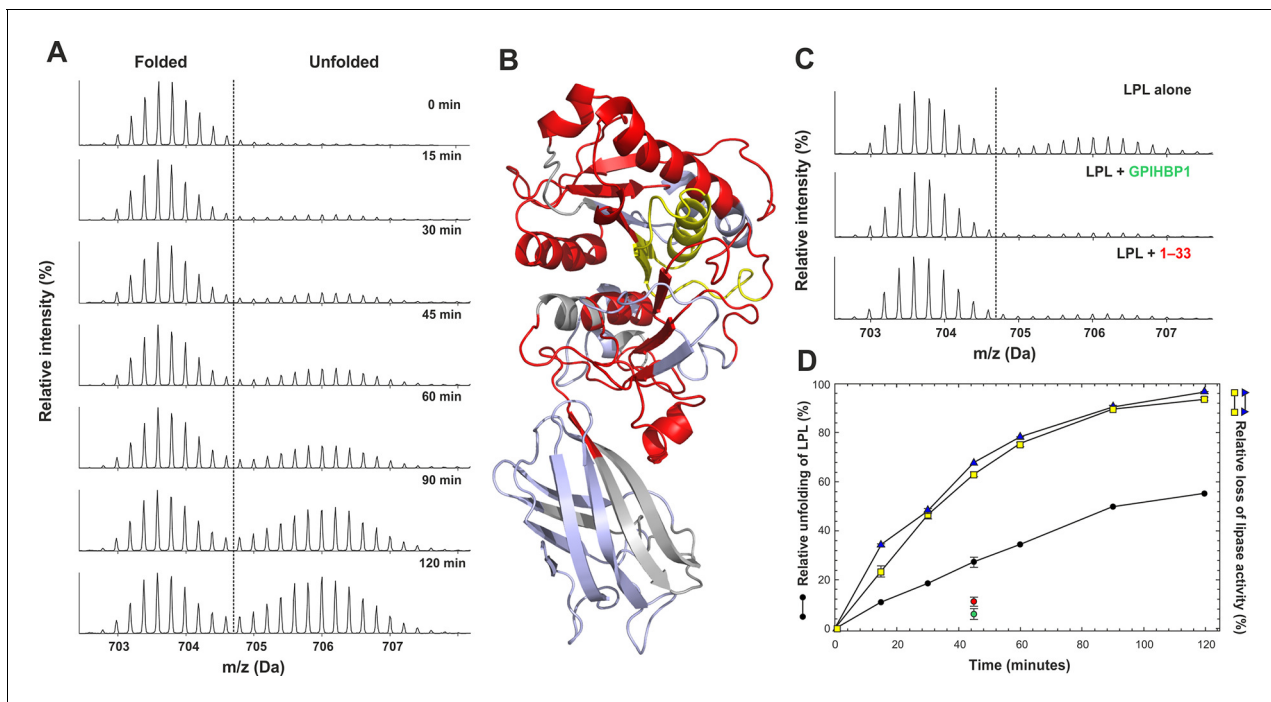
**Figure 4.** Kinetic assessment of the GPIHBP1•LPL interaction by single-cycle titration SPR. The basic principles in the single-cycle kinetic titration are illustrated in panel A. Initially, LPL is captured in a noncovalent fashion on the CM4 sensor surface after a 150 s injection of 200 nM of purified LPL across the flow cell containing immobilized mAb 5D2. After a 600 s stabilization period, a series of five 90 s pulses with increasing analyte concentration are injected without intervening regeneration. The following concentrations of either mAb 4-1a (A), mAb 5D2 (A), GPIHBP1<sup>1-131</sup> (B), or GPIHBP1<sup>34-131</sup> (C) were analyzed: 12.5, 25, 50, 100, and 200 nM. Panels B and C shows the buffer referenced sensorgrams recorded for GPIHBP1<sup>1-131</sup> and GPIHBP1<sup>34-131</sup>, respectively. The mathematical fitting to a simple 1:1 binding model are superimposed as red lines and the residuals are shown in green. LPL, lipoprotein lipase; SPR, surface plasmon resonance.

DOI: [10.7554/eLife.12095.012](https://doi.org/10.7554/eLife.12095.012)



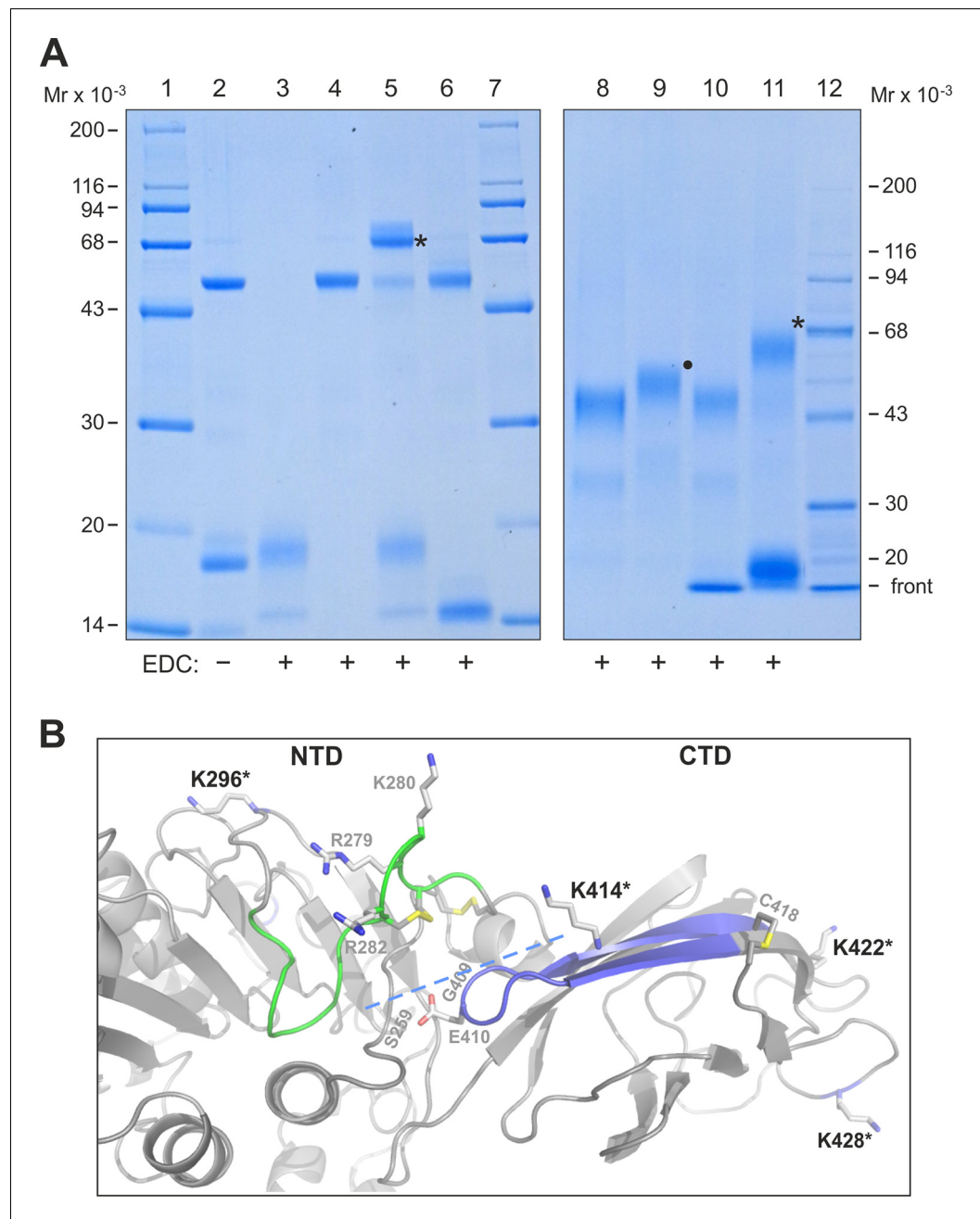
**Figure 5.** Equilibrium binding constants of the GPIHBP1•LPL interaction by microscale thermophoresis. The microscale thermophoresis signals for the interaction of LPL with 5 nM Alexa Fluor-647-labeled GPIHBP1<sup>1-131/R38G</sup> (panel A) and GPIHBP1<sup>34-131/R38G</sup> (panel B) were recorded in quadruplicates for two-fold dilution series of unlabeled  $\text{LPL}_2$  (10 pM to 350 nM). The mean values and standard deviation for the thermophoresis are shown as well as a fitting to a 1:1 binding model (software supplied with Monolith NT.115). LPL, lipoprotein lipase.

DOI: [10.7554/eLife.12095.013](https://doi.org/10.7554/eLife.12095.013)



**Figure 6.** Progressive unfolding of LPL as determined by HDX-MS. Panel A shows the unfolding of the catalytic domain of LPL when incubated at 25°C. The unfolding is evident from the appearance of a bimodal isotopic envelope for the peptide 131–165, which contains Ser<sup>134</sup> and Asp<sup>158</sup> of the catalytic triad. Panel B shows the global distribution of peptides in the catalytic domain that undergo unfolding (in red). The peptide 131–165 is highlighted in yellow. Peptides that are not exhibiting bimodal isotope envelopes are colored light blue; segments of LPL not recovered by the HDX-MS are colored gray. The impact of GPIHBP1<sup>1–131</sup> and the N-terminal acidic peptide GPIHBP1<sup>1–33</sup> on LPL unfolding is shown in panel C. In these studies, equimolar amounts of GPIHBP1<sup>1–131</sup> or GPIHBP1<sup>1–33</sup> (relative to the LPL<sub>2</sub>) inhibited unfolding of the NTD of LPL. The progressive unfolding of LPL was quantified by fitting two Gaussian distributions to the isotopic envelopes of peptide 131–165 representing the folded and unfolded states (panel A) and is shown in panel D (black circles). Unfolding at the 45-min incubation time point was measured in triplicates with and without equimolar amounts of GPIHBP1<sup>1–131</sup> (green circle) or GPIHBP1<sup>1–33</sup> (red circle). The progressive loss of triolein hydrolase and esterase activities of LPL were recorded in parallel as a time-dependent function of pre-incubating 2 μM LPL<sub>2</sub> under identical conditions and is shown by the yellow squares and blue triangles, respectively. LPL, lipoprotein lipase; HDX-MS, hydrogen–deuterium exchange mass spectrometry; NTD, N-terminal domain

DOI: 10.7554/eLife.12095.014



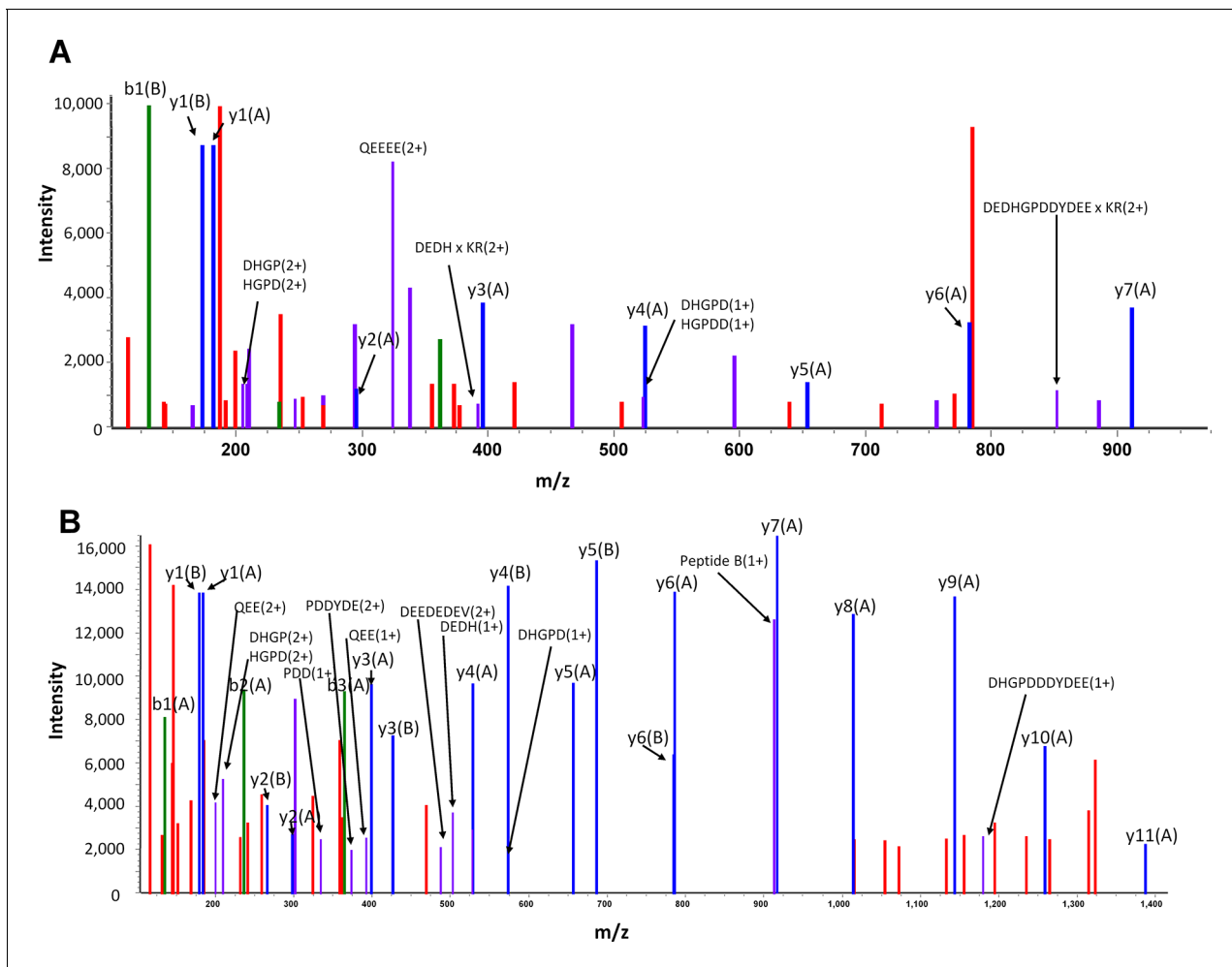
**Figure 7.** Zero-length cross-linking of GPIHBP1<sup>1–131</sup> and GPIHBP1<sup>1–33</sup> to bovine LPL. Panel **A**, left shows a Coomassie Blue–stained 12% polyacrylamide gel after SDS–PAGE analysis of reduced and alkylated samples representing various combinations of 1.5  $\mu$ M LPL<sub>2</sub> and 7  $\mu$ M GPIHBP1 variants subjected to EDC cross-linking. Lane 2 shows LPL GPIHBP1<sup>1–131</sup> before cross-linking. Lanes 3–6 show samples after EDC cross-linking: GPIHBP1<sup>1–131</sup> (lane 3); LPL (lane 4), LPL GPIHBP1<sup>1–131</sup> (lane 5), and LPL GPIHBP1<sup>34–131</sup> (lane 6). The covalently bound conjugate representing LPL•GPIHBP1<sup>1–131</sup> is marked by an asterisk. Right panel shows a Coomassie Blue–stained 4–12% gradient polyacrylamide gel after analysis of EDC cross-linked 3  $\mu$ M LPL<sub>2</sub> alone (lane 8) or in the presence of 15  $\mu$ M GPIHBP1<sup>1–33</sup> (lane 9); 15  $\mu$ M GPIHBP1<sup>34–131</sup> (lane 10); and 15  $\mu$ M GPIHBP1<sup>1–131</sup> (lane 11). The covalent conjugates representing LPL•GPIHBP1<sup>1–131</sup> and LPL•GPIHBP1<sup>1–33</sup> are indicated by an asterisk and a solid dot, respectively. Molecular weight markers are shown in lanes 1, 7 & 12. Panel **B** shows a model of human LPL highlighting the cross-linking sites in GPIHBP1 that were identified by MS (asterisks). Areas that have been assigned as potential interaction sites for GPIHBP1 by HDX–MS are shown in green (for the acidic domain of GPIHBP1) and blue (for the LU domain of GPIHBP1). The position of the interdomain interface in LPL between the NTD and CTD is marked by a dashed line, and three residues within this interface linked to familial

Figure 7 continued on next page

*Figure 7 continued*

chylomicronemia when mutated (S259R, G409R, and E410V) are shown by gray numbers. Basic residues of the heparin-binding site in the catalytic domain of LPL (R279, K280, R282) are shown as sticks. Note, bovine LPL contains two additional residues compared with human LPL, for example Lys<sup>296</sup> in human LPL is equivalent to Lys<sup>298</sup> in bovine LPL. CTD, C-terminal domain; EDC, N-ethyl-N'-[3-(diethylamino)propyl]-carbodiimide; HDX-MS, hydrogen-deuterium exchange mass spectrometry; LPL, lipoprotein lipase; MS, mass spectrometry; NTD, N-terminal domain; SDS-PAGE, sodium dodecyl sulfate polyacrylamide gel electrophoresis.

DOI: [10.7554/eLife.12095.016](https://doi.org/10.7554/eLife.12095.016)



**Figure 7—figure supplement 1.** Fragment spectra identifying EDC-mediated inter-domain cross-links in mature LPL•GPIHBP1<sup>1–131</sup> complexes. Panel A shows the fragment spectra produced for the EDC cross-linked peptide between residues 1–33 in GPIHBP1 and residues 295–299 (VARKR) in bovine LPL. Panel B shows the fragment spectra produced for the cross-linked peptide between residues 1–33 in GPIHBP1 and residues 416–422 (KVIFCSR) in bovine LPL. Fragments derived from residues 1–33 of GPIHBP1 are designated (A) and peptides from LPL are designated (B). The blue peaks correspond to y-fragment ions from either peptide; green peaks correspond to b-fragments ions from either peptide; red peaks represent unassigned peaks; purple peaks correspond to loss of NH<sub>3</sub> or H<sub>2</sub>O (not labeled) or ions that have undergone two fragmentation reactions. Peaks corresponding to cross-linked peptide fragments are assigned by an x along with the two peptide fragments (e.g. DEDHxKR). EDC, N-ethyl-N'-[3-diethylamino)propyl]-carbodiimide; LPL, lipoprotein lipase.

DOI: [10.7554/eLife.12095.017](https://doi.org/10.7554/eLife.12095.017)

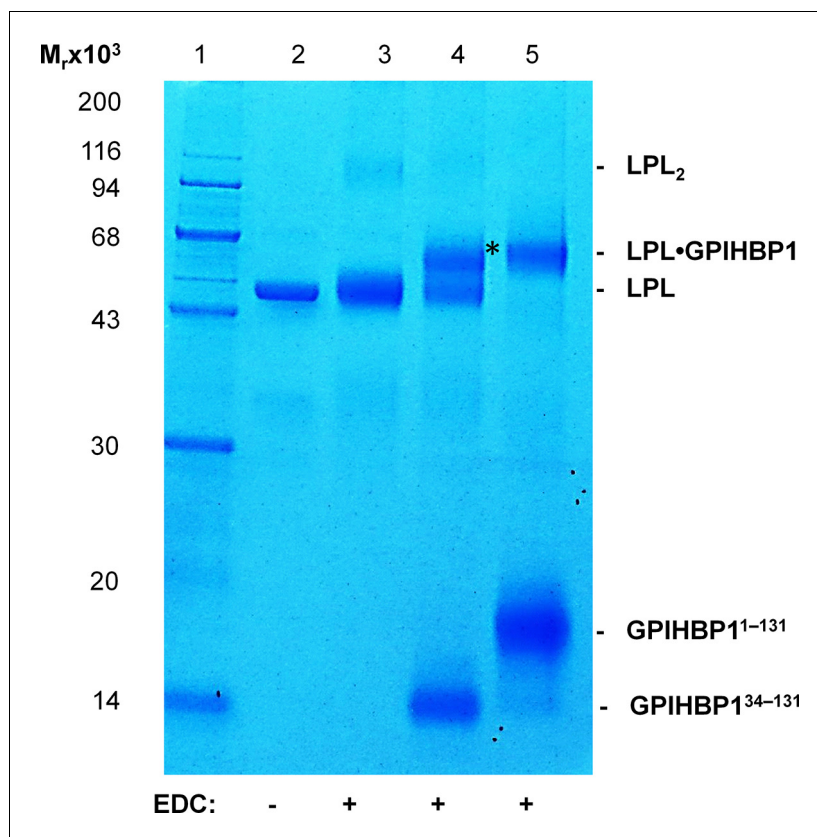


**Figure 7—figure supplement 2.** SDS-PAGE analysis of EDC/NHS cross-linked LPL•GPIHBP1 complexes. The cross-linking efficiencies between LPL and GPIHBP1<sup>34–131</sup> or GPIHBP1<sup>1–131</sup> are revealed by a Coomassie Blue–stained 12% SDS-polyacrylamide gel. The samples were cross-linked for 4 hr by 5 mM EDC and NHS in the following format: 3  $\mu$ M LPL<sub>2</sub> alone (*lane 3*) or in the presence of 15  $\mu$ M GPIHBP1<sup>34–131</sup> (*lane 4*) or 15  $\mu$ M GPIHBP1<sup>1–131</sup> (*lane 5*). LPL without EDC/NHS is shown in *lane 2*. Molecular mass markers are in *lane 1*. The asterisk shows a covalent LPL•GPIHBP1<sup>34–131</sup> conjugate. Using these cross-linking conditions, we observe a low level of covalently-linked LPL dimers (*lane 3*); the amount of these LPL dimers is reduced by the presence of GPIHBP1<sup>34–131</sup> or GPIHBP1<sup>1–131</sup> (*lane 4* & *lane 5*), likely reflecting the engagement of LPL in interactions with these ligands.

EDC, N-ethyl-N'-[3-diethylamino)propyl]-carbodiimide; LPL, lipoprotein lipase; NHS, N-hydroxysuccinimide; SDS-PAGE, sodium dodecyl sulfate polyacrylamide gel electrophoresis.

DOI: [10.7554/eLife.12095.018](https://doi.org/10.7554/eLife.12095.018)